Available online at www.sciencedirect.com
ScienceDirect
Phytochemistry 68 (2007) 652–662
PHYTOCHEMISTRY
www.elsevier.com/locate/phytochem

Covalent anthocyanin–flavone dimer from leaves of *Oxalis triangularis*

Torgils Fossen [a,*], Saleh Rayyan [a], Maya H. Holmberg [a], Manfred Nimtz [b], Øyvind M. Andersen [a]

[a] *Department of Chemistry, University of Bergen, Allégt. 41, N-5007 Bergen, Norway*
[b] *Helmholz Centre for Infection Research, Department of Structural Biology, Inhoffenstrasse 7, D-38124 Braunschweig, Germany*

Received 20 July 2006; received in revised form 30 October 2006
Available online 19 December 2006

Abstract

The anthocyanin–flavone *C*-glycoside, (malvidin 3-*O*-(6^{II}-*O*-α-rhamnopyranosyl^{AIV}-β-glucopyranoside^{AII})-5-*O*-β-glucopyranoside^{AIII}) (apigenin 6-*C*-(2^{II}-*O*-β-glucopyranosyl^{FIII}-β-glucopyranoside^{FII})) malonate^{AV} (A^{IV}-4 → A^{V}-1, F^{III}-6 → A^{V}-3) (**1**), has been isolated from leaves of *Oxalis triangularis* A. St.-Hil. In the 1D ^{1}H NMR spectrum of **1** dissolved in CD_3OD–CF_3CO_2D (95:5), MTFA, recorded 45 min after sample preparation, this covalently linked dimer occurred mainly as flavylium cation (38%) and two equilibrium forms assigned to be quinonoidal bases (54%), whereas only minor amounts of the hemiacetal forms were present. After five days storage at 300 K, the hemiacetals (39%) and flavylium cation (38%) constituted the main forms of **1**. More simple anthocyanins are normally considered to be on the flavylium cation form in acidified deuterated methanol. The cross-peaks observed in NOESY NMR spectra of **1** indicated the presence of vertical 'π–π' stacking between the B-ring of the flavone unit and the A-ring of each of the two forms assigned to be quinonoidal bases. It was not possible to discriminate between inter- or intramolecular association mechanisms. The equilibria between the various forms of **1** were studied by two-dimensional NOESY and ROESY NMR spectroscopy. 2D HSQC-TOCSY NMR spectroscopy was among the methods used for characterization of the various forms.

Keywords: *Oxalis triangularis*; Leaves; Anthocyanin–flavone *C*-glycoside dimer; Malvidin 3-rutinoside-5-glucoside (malonate) apigenin 6-*C*-sophoroside; Colour; Equilibrium forms; HSQC-TOCSY; ^{13}C NMR

1. Introduction

More than 34% of the reported anthocyanins have been found to be acylated with aliphatic acyl moieties (Andersen and Jordheim, 2006). Dicarboxylic acids, among which malonic acid is the most common type (25%), make possible a covalent linkage between the anthocyanin and another flavonoid unit through the dicarboxylic acid. Covalently linked anthocyanin–flavonol pigments have been isolated from blue flowers of *Agapanthus* (Bloor and Falshaw, 2000) and from pale-purple flowers of chive (Fossen et al., 2000), while disubstituted dicarboxylic acids involving an anthocyanin and a flavone have been isolated from the blue-violet flowers of *Eichhornia crassipes* (Pontederiaceae) (Toki et al., 1994, 2004). These structures were established as (6^{III}-*O*-(delphinidin 3-*O*-(6^{II}-*O*-(β-D-glucopyranosyl)-β-D-glucopyranosyl))) (6^{II}-*O*-(apigenin 7-*O*-(β-D-glucopyranosyl))) malonate and its corresponding luteolin derivative. The existence of other anthocyanin-flavonol complexes has been indicated in orchids (Strack et al., 1989), lupins (Takeda et al., 1993) and *Salvia patens* (Takeda et al., 1994).

Anthocyanidins are reckoned to be involved in a series of equilibria giving rise to different forms, which exhibit their own properties including colour (Brouillard and Dangles, 1994). One- and two-dimensional ^{1}H NMR have to some extent been used to characterize the various forms of the 3-glucoside and 3,5-diglucoside of malvidin present in acidic aqueous solutions, and to determine their molar

* Corresponding author. Tel.: +47 55 58 82 44; fax: +47 55 58 94 90.
E-mail address: Torgils.Fossen@kj.uib.no (T. Fossen).

0031-9422/$ - see front matter © 2006 Elsevier Ltd. All rights reserved.
doi:10.1016/j.phytochem.2006.10.030

fractions as a function of pH (Hoshino et al., 1982; Cheminat and Brouillard, 1986; Hoshino, 1991; Mistry et al., 1991; Santos et al., 1993). Vitisin A has been assumed to be formed from malvidin 3-glucoside by condensation reaction with pyruvic acid in red wine during storage (Bakker et al., 1997; Fulcrand et al., 1998). Several forms, including hemiacetals, quinonoidal bases, chalcones and the flavylium cation form were tentatively identified when vitisin A was dissolved in DMSO-d_6–TFA-*d* (9:1; v/v) (Bakker et al., 1997). Increasing proportions of the chalcone forms and decreasing proportions of the flavylium form, respectively, were observed during storage, suggesting that the chalcone forms were favourable under these solvent conditions. The flavylium cation and chalcone forms of vitisin A were partly characterised by ^{1}H and ^{13}C NMR spectroscopy (Bakker et al., 1997). In acidified methanolic solutions and in aqueous solutions at pH lower than 5-6, pyranoanthocyanins like vitisin A have been reported to occur mainly as flavylium cations (Bakker and Timberlake, 1997; Fulcrand et al., 1998; Fossen and Andersen, 2003). The only previously reported complete assignment of ^{1}H and ^{13}C NMR chemical shifts of another anthocyanin equilibrium form than the flavylium cation form, described one 2-OH hemiacetal form of malvidin 3-*O*-(6^{II}-*O*-(*E*)-*p*-coumaroyl-β-D-glucopyranosyl)-5-*O*-(2-*O*-acetyl-β-D-xyloopyranoside), isolated from *Tibouchina urvilleana* flowers, using DMSO-d_6–TFA-*d* (9:1; v/v) as solvent (Terahara and Suzuki, 1993).

Anthocyanins in solutions can be stabilized by: (i) copigmentation with other aromatics like flavones and cinnamic acids, (ii) intramolecular sandwich 'π–π' stacking of the anthocyanidin and aromatic acyl residues of anthocyanins di- or poly-acylated with aromatic acyl groups and (iii) intermolecular self-association by vertical hydrophobic 'π–π' stacking of the aromatic anthocyanidin nuclei (Hoshino et al., 1982; Goto et al., 1987; Goto and Kondo, 1991; Hoshino, 1991, 1992; Nerdal and Andersen, 1991, 1992; Kondo et al., 1998; Gakh et al., 1998). Based on circular dichroism (CD) spectroscopy, 1D ^{1}H NMR spectra recorded at different temperatures and with various anthocyanin concentrations (Hoshino et al., 1982; Hoshino, 1991, 1992), and NOESY NMR cross-peaks obtained at different temperatures (Nerdal and Andersen, 1991, 1992), intermolecular self-association has been reported for the anhydrobase equilibrium forms occurring in weakly acidic–neutral aqueous solvents and for the flavylium cation in acidified methanol, respectively. Based on distance geometry calculations self-association structures were proposed (Nerdal and Andersen, 1991, 1992). The impact of inter- or intra-molecular copigmentation in covalent anthocyanin–flavone and anthocyanin–flavonol pigments on flower colour, has to some extent been discussed previously (Figueiredo et al., 1996; Bloor and Falshaw, 2000; Fossen et al., 2000; Toki et al., 1994, 2004).

In this paper, we report the isolation and identification of a novel covalently linked anthocyanin–flavone *C*-glycoside, **1** (Fig. 1), isolated from leaves of *Oxalis triangularis*. When dissolved in acidified methanol, **1** occurred in various equilibrium forms depending on storage time, and one aim of this paper was to characterize these forms by both ^{1}H and ^{13}C NMR spectroscopy. Some considerations regarding intra- or intermolecular association of **1** are reported.

2. Results and discussion

The aqueous concentrate of the acidified methanolic extract of leaves of *O. triangularis* was purified by partition against ethyl acetate followed by Amberlite XAD-7 column chromatography. Pigment **1** co-eluted (HPLC) with malvidin 3-*O*-(6-*O*-(4-*O*-malonyl-α-rhamnopyranosyl-β-glucopyranoside)-5-*O*-β-glucopyranoside (Table 1), which is one of the main anthocyanins of *O. triangularis*, thus preventing the detection of **1** in the crude extract. However, **1** was separated from the monomeric anthocyanins by Sephadex LH-20 chromatography, and thereafter purified by preparative HPLC. The UV–Vis spectrum of **1** recorded on-line during HPLC analysis (Fig. 2) showed visible maximum at 558 nm, the $A_{440}/A_{\text{vis-max}}$ ratio of 10%, and local UV maxima at 346 nm, 310 nm and 276 nm, respectively, indicating both a 3,5-disubstituted anthocyanin and another flavonoid unit. Analysis of the NMR spectra of **1** recorded in CF_3COOD–CD_3OD (5:95; v/v) revealed that **1** existed in several equilibrium forms (denoted as **1b**–**1e**) in addition to the flavylium cation form, **1a** (Figs. 3 and 4). The equilibria between the different forms of **1**, and potential inter- or intramolecular associations of **1**, were examined by 2D nuclear Overhauser and exchange spectroscopy (NOESY) and rotational frame nuclear Overhauser effect (ROESY) spectroscopy performed at 271 K and 300 K. The relative proportions of the various equilibrium forms of **1** in the NMR solvent varied with storage time.

2.1. The flavylium cation form, *1a*

The downfield regions of the 1D ^{1}H NMR, ^{1}H–^{13}C HMBC and ^{1}H–^{13}C HSQC spectra of **1** showed signals in agreement with both malvidin and *C*-substituted apigenin (Table 2). The diagnostic ^{13}C chemical shift value of C-8F (δ 93.1) revealed 6-C substitution (Rayyan et al., 2005) of the apigenin moiety. A molecular ion (M^+) at *m*/*z* 1463.36 in the positive ion ESI mass spectrum was in accordance with covalently linked malvidin, apigenin, malonyl, rhamnosyl and four hexoses.

The anomeric coupling constants (7.7 Hz, 7.7 Hz, 7.7 Hz, 10.3 Hz and 1.5 Hz), the ^{13}C resonances in the sugar region of the 2D ^{1}H–^{13}C HSQC spectrum, and the cross-peaks in the ^{1}H–^{1}H DQF-COSY, the ^{1}H–^{1}H TOCSY and the ^{1}H–^{13}C HSQC-TOCSY spectra of **1** (Fig. 5) were in agreement with four β-glucopyranoses and one α-rhamnopyranose (Fossen and Andersen, 2006) (Table 2). The anomeric carbon at δ 73.4, its $^3J_{HH}$ of 10.3 Hz, and

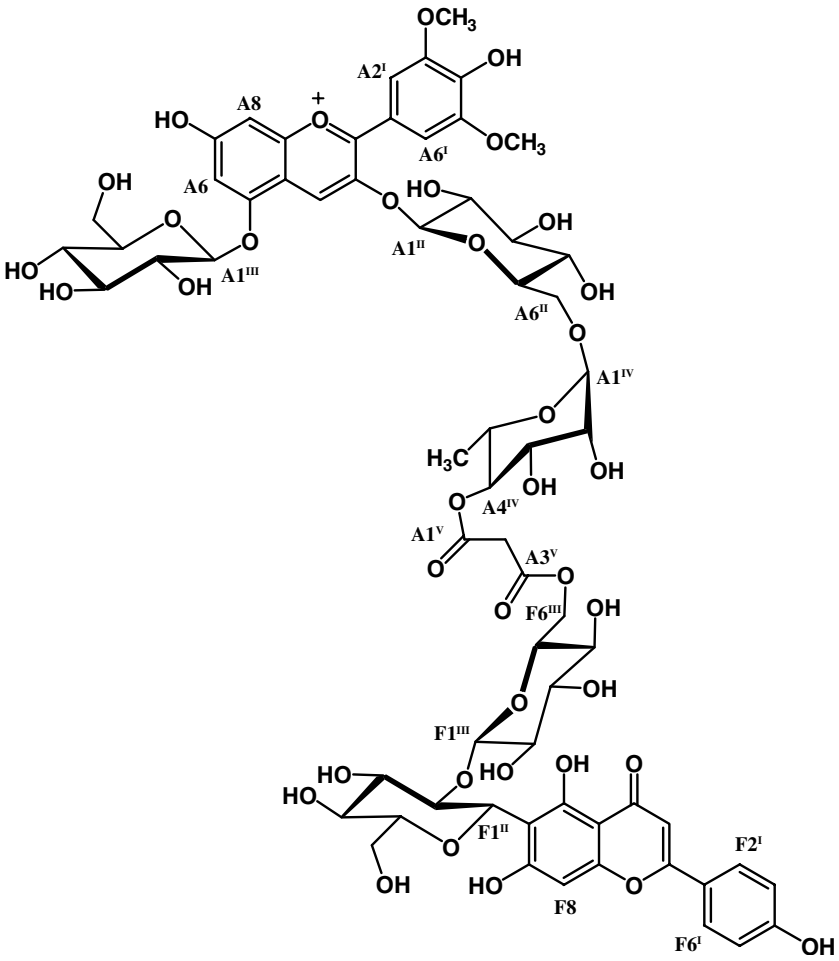

Fig. 1. Structure and nomenclature of (malvidin 3-*O*-(6^{II}-*O*-α-rhamnopyranosyl^{AIV}-β-glucopyranoside^{AII})-5-*O*-β-glucopyranoside^{AIII}) (apigenin 6-*C*-(2^{II}-*O*-β-glucopyranosyl^{FIII}-β-glucopyranoside^{FII}) malonate^{AV} (A^{IV}-4 → A^{V}-1, F^{III}-6 → A^{V}-3), **1**.

Table 1
Chromatographic (HPLC) and spectral (UV–Vis and MS) data recorded for (malvidin 3-*O*-(6^{II}-*O*-α-rhamnopyranosyl^{AIV}-β-glucopyranoside^{AII})-5-*O*-β-glucopyranoside^{AIII}) (apigenin 6-*C*-(2^{II}-*O*-β-glucopyranosyl^{FIII}-β-glucopyranoside^{FII}) malonate^{AV} (A^{IV}-4 → A^{V}-1, F^{III}-6 → A^{V}-3) (**1**) and the monomeric anthocyanins malvidin 3-*O*-(6^{II}-*O*-α-rhamnopyranosyl-β-glucopyranoside)-5-*O*-β-glucopyranoside (**2**) and malvidin 3-*O*-(6^{II}-*O*-(4^{IV}-*O*-malonyl-α-rhamnopyranosyl-β-glucopyranoside)-5-*O*-β-glucopyranoside (**3**) isolated from leaves of *Oxalis triangularis*

Compound	On-line HPLC						ESI-MS
	Vis_{max} (nm)	UV_{max} (nm)	$A_{440}/A_{vis\text{-}max}$ (%)	$A_{320}/A_{vis\text{-}max}$ (%)	$A_{UV\text{-}max}/A_{vis\text{-}max}$ (%)	t_R (min)	M^+ *m/z*
1	558	276	10	43	77 ($A_{276}/A_{vis\text{-}max}$)	16.55	1463.36
		310			44 ($A_{310}/A_{vis\text{-}max}$)		
		346			55 ($A_{346}/A_{vis\text{-}max}$)		
2	530	278	14	13	104	15.63	801.245
3	533	278	11	10	87	16.42	887.249

M^+, molecular ion.

the remaining ^{13}C signals belonging to this sugar unit were in accordance with a *C*-glucopyranose. The downfield chemical shift of H-2^{II}F (δ 4.43), and the crosspeak at δ 4.43/4.49 (H-2^{II}F/H-1^{III}F) in the NOESY spectrum (Fig. 6), showed the interglycosidic linkage to be in agreement with the disaccharide sophorose. The downfield chemical shift of C-6^{III}F (64.6) and the crosspeak at δ 4.07/165.4 (H-6B^{III}F/C-3 malonyl) in the HMBC-spectrum (Fig. 6) confirmed the linkage position of the malonyl. The crosspeaks at δ 5.57/146.0 (H-1^{II}A/C-3A) and δ 5.27/156.4 (H-1^{III}A/C-5A) in the HMBC spectrum (Fig. 6), in addition to the crosspeaks at δ 5.57/9.06 (H-1^{II}A/H-4A) and δ 5.27/7.13 (H-1^{III}A/H-6A) in the NOESY spectrum (Fig. 6) revealed the linkages between malvidin and the remaining two glucose units to be at the 3- and 5-positions, respectively. The crosspeaks at δ 4.76/67.8 (H-1^{IV}A/C-6^{II}A) and δ 3.75/102.2 (H-6B^{II}A/C-1^{IV}A) in the HMBC spectrum (Fig. 6) and the crosspeaks at δ 4.76/4.10

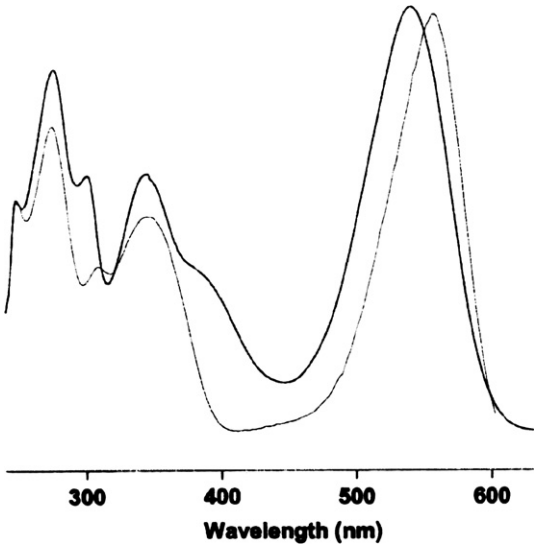

Fig. 2. UV–Vis spectra of (malvidin 3-*O*-(6^{II}-*O*-α-rhamnopyranosyl^{AIV}-β-glucopyranoside^{AII})-5-*O*-β-glucopyranoside^{AIII}) (apigenin 6-*C*-(2^{II}-*O*-β-glucopyranosyl^{FIII}-β-glucopyranoside^{FII}) malonate^{AV} (A^{IV}-4 → A^{V}-1, F^{III}-6 → A^{V}-3), **1** recorded on-line during HPLC analysis (dashed line) and in 0.01% HCl–MeOH (bold line).

(H-1^{IV}A/H-6A^{II}A) and δ 4.76/3.75 (H-1^{IV}A/H-6B^{II}A) in the NOESY spectrum (Fig. 6) revealed the interglycosidic linkage to be in agreement with the disaccharide rutinose. The downfield shift of H-4^{IV}A (δ 4.87) and the crosspeak at δ 4.87/167.2 (H-4^{IV}A/C-1 malonyl) in the HMBC-spectrum (Fig. 6) confirmed the malonyl to be linked to the rhamnosyl 4-position. Thus, **1** was identified as (malvidin 3-*O*-(6^{II}-*O*-α-rhamnopyranosyl^{AIV}-β-glucopyranoside^{AII})-5-*O*-β-glucopyranoside^{AIII}) (apigenin 6-*C*-(2^{II}-*O*-*β*-glucopyranosyl^{FIII}-β-glucopyranoside^{FII}) malonate^{AV} (A^{IV}-4 → A^{V}-1, F^{III}-6 → A^{V}-3) (Fig. 1). Daughter ions at *m/z* 1301.30, 1031.27, 887.29, 869.21, 655.17, 493.12, 433.10, 415.09 and 331.07 obtained in the positive ion ESI mass spectrum after collision induced dissociation (CID) of the parent ion (*m/z* 1463.36), corresponding to M – 5-glucose, M – apigenin 6-*C*-glucoside, malvidin 3-*O*-(6^{II}-*O*-(4^{IV}-*O*-malonylrhamnosyl)glucoside)-5-*O*-glucoside, M – apigenin diglucoside, malvidin 3,5-*O*-diglucoside, malvidin glucoside, apigenin 6-*C*-glucoside – H_2O, and malvidin, respectively, confirmed this identity.

2.2. The hemiacetal forms, *1b* and *1c*

The equilibrium of the flavylium cation form (**1a**) with the hemiacetal forms (**1b** and **1c**) of **1** (Fig. 3) was confirmed by observation of strong exchange peaks between analogous protons of each form in the NOESY spectrum. The ROESY experiments were particularly useful to distinguish exchange crosspeaks (positive) from rotational frame Overhauser effect (ROE) and transfer rotational frame Overhauser effect (trROE) crosspeaks (negative). The exchange peaks in the NOESY spectrum between the protons of **1a** and the corresponding protons of **1b** and **1c** at δ 9.06/6.72 (**1a**H-4A/**1b**H-4A), δ 9.06/6.71 (**1a**H-4A/**1c**H-4A), δ 8.11/6.95 (**1a**H-2^{I},6^{I}A/**1b**H-2^{I},6^{I}A), δ 8.11/6.94 (**1a**H-2^{I},6^{I}A/**1c**H-2^{I},6^{I}A), δ 7.24/6.22 (**1a**H-8A/**1b**H-8A), δ 7.24/6.20 (**1a**H-8A/**1c**H-8A), δ 7.13/6.39 (**1a**H-6A/**1b**H-6A), δ 7.13/6.37 (**1a**H-6A/**1c**H-6A), δ 4.09/3.90 (**1a**OCH$_3$A/**1b**OCH$_3$A), δ 4.09/3.89 (**1a**OCH$_3$A/**1c**OCH$_3$A), δ 5.57/5.09 (**1a**H-1^{II}A/**1b**H-1^{II}A), δ 5.57/5.01 (**1a**H-1^{II}A/**1c**H-1^{II}A), δ 3.78/3.37 (**1a**H-2^{II}A/**1b**H-2^{II}A), δ 3.78/3.40 (**1a**H-2^{II}A/**1c**H-2^{II}A), δ 3.53/3.31 (**1a**H-4^{II}A/**1b**H-4^{II}A), δ 5.27/4.98 (**1a**H-1^{III}A/**1b**H-1^{III}A), δ 5.27/4.95 (**1a**H-1^{III}A/**1c**H-1^{III}A), δ 4.76/4.87 (**1a**H-1^{IV}A/**1b**H-1^{IV}A), δ 3.90/3.71 (**1a**H-5^{IV}A/**1b**H-5^{IV}A) and δ 0.99/1.04 (**1a**H-6^{IV}A/**1b**H-6^{IV}A)

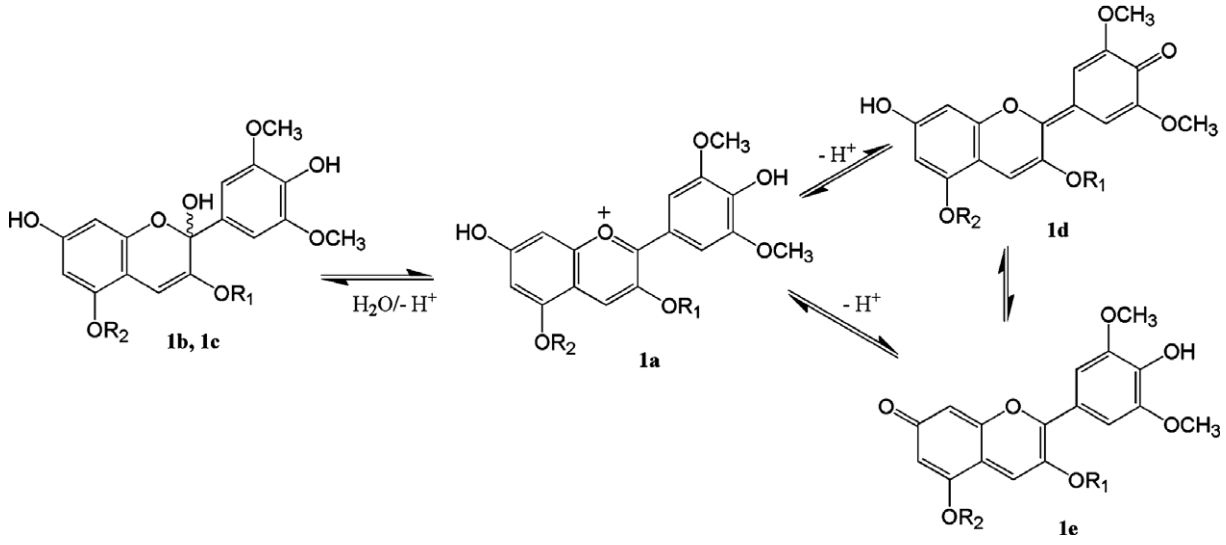

Fig. 3. Structure of the anthocyanidins of the equilibrium forms of (malvidin 3-*O*-(6^{II}-*O*-α-rhamnopyranosyl^{AIV}-β-glucopyranoside^{AII})-5-*O*-β-glucopyranoside^{AIII}) (apigenin 6-*C*-(2^{II}-*O*-β-glucopyranosyl^{FIII}-β-glucopyranoside^{FII}) malonate^{AV} (A^{IV}-4 → A^{V}-1, F^{III}-6 → A^{V}-3), **1** detected in CF_3COOD–CD_3OD (5:95; v/v) at 300 K. **1d** and **1e** are indicated to be quinonoidal bases, however, assignment of their ^{1}H and ^{13}C NMR signals is incomplete because of significant broadening of their signals in the NMR spectra.

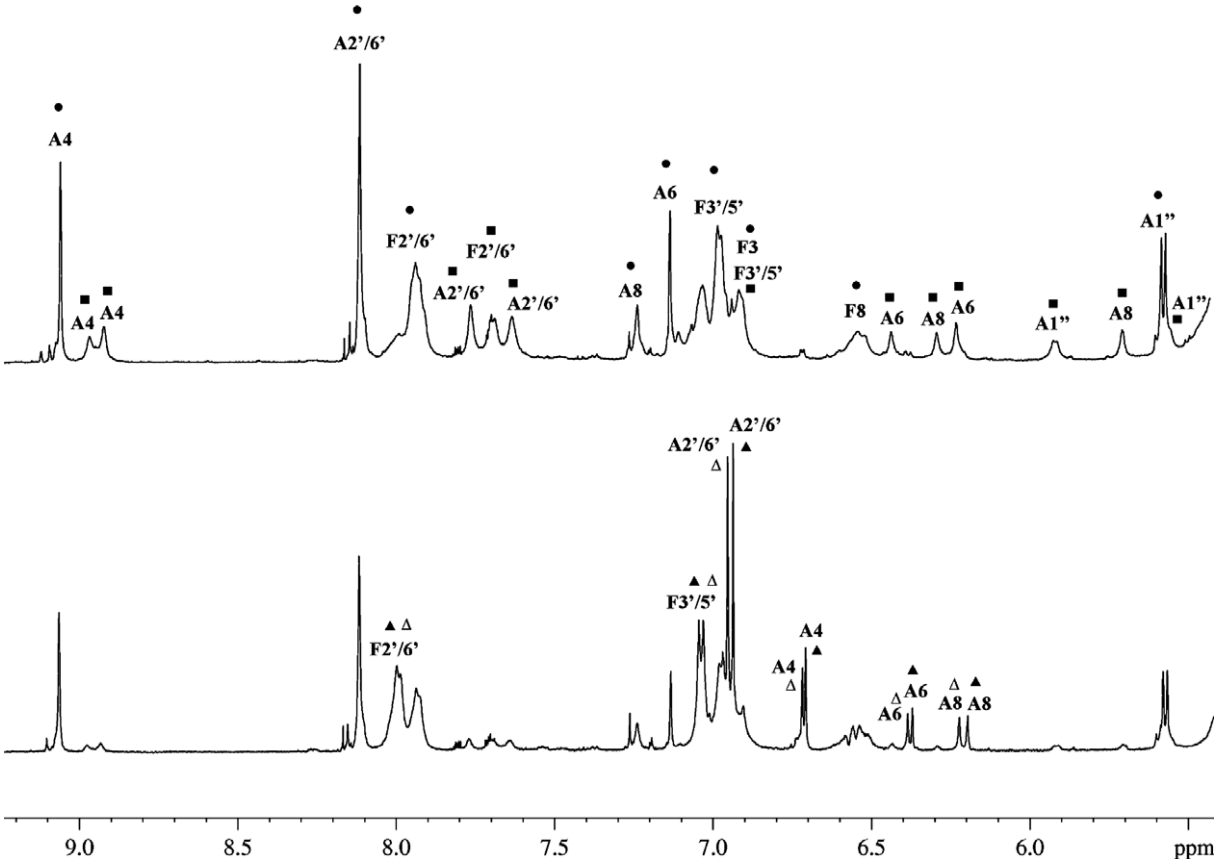

Fig. 4. Expanded region of 1D ^{1}H NMR spectra of (malvidin 3-*O*-(6^{II}-*O*-α-rhamnopyranosyl^{AIV}-β-glucopyranoside^{AII})-5-*O*-β-glucopyranoside^{AIII}) (apigenin 6-*C*-(2^{II}-*O*-β-glucopyranosyl^{FIII}-β-glucopyranoside^{FII}) malonate^{AV} (A^{IV}-4 → A^{V}-1, F^{III}-6 → A^{V}-3), **1** dissolved in CF_3COOD–CD_3OD (5:95; v/v) at 300 K. Top: spectrum recorded 1 h after sample preparation. Bottom: recorded 5 days after sample preparation. Circles denote the flavylium form, squares denote the forms assigned to quinonoidal bases, and black and white triangles denote the major and minor hemiacetal forms, respectively.

were of special importance for revealing the equilibrium of **1a** with **1b** and **1c**, respectively. The ^{1}H and ^{13}C resonances of **1b** and **1c** (Table 3) were assigned from the 1D ^{1}H and 2D HSQC-TOCSY, HSQC, HMBC, COSY, TOCSY, NOESY, and ROESY NMR experiments to be in accordance with two 2-hydroxylated enantiomeric hemiacetal forms of **1**. These spectra were recorded after 5–14 days storage, when the hemiacetal forms were main equilibrium forms of **1** (Fig. 7). The ^{1}H chemical shifts of **1b** and **1c** (Table 3) were relatively similar to analogous chemical shift values reported for carbinol pseudobases (hemiacetal) forms of malvin (Hoshino, 1991; Santos et al., 1993), and the ^{13}C NMR chemical shifts of the aglycones of **1b** and **1c** were relatively similar to analogous chemical shifts of the single reported 2-OH hemiacetal form of malvidin 3-O-(6^{II}-*O*-(*E*)-*p*-coumaroyl-β-D-glucopyranosyl)-5-*O*-(2-*O*-acetyl-β-D-xyloopyranoside) (Terahara and Suzuki, 1993).

2.3. The equilibrium forms *1d* and *1e*

In addition to the flavylium (**1a**) and hemiacetal forms (**1b** and **1c**) the presence of two other forms of **1** (**1d** and **1e**) was detected in the NMR spectra of **1** (Table 4). The downfield chemical shifts of **1d**H-4A (δ 8.97), **1e**H-4A (δ 8.92), **1d**C-4A (δ 133.0) and **1e**C-4A (δ 131.0), respectively, observed in the 1D ^{1}H and the 2D ^{1}H–^{13}C HSQC spectra, respectively, indicated that the C-rings of these forms were conjugated, most probably in accordance with two quinonoidal base forms (Fig. 3). The exchange peaks observed in the NOESY and ROESY spectra at δ 6.43/6.22 (**1d**H-6A/**1e**H-6A), δ 6.29/5.71 (**1d**H-8A/**1e**H-8A), δ 7.77/7.64 (**1d**H-2′,6′A/**1e**H-2′,6′A), δ 5.91/5.56 (**1d**H-1″/**1e**H-1″) and δ 7.69/7.92 (**1d**H-2′,6′F/**1e**H-2′,6′F), confirmed the equilibrium between **1d** and **1e**. Exchange peaks for the direct equilibrium between the flavylium form and **1d** and **1e**, respectively, could not be detected in the NMR spectra recorded at 271 K and 300 K. However, weak exchange peaks were identified at δ 8.97/6.74 (**1d**H-4A/**1b**H-4A,**1c**H-4A), and δ 8.92/6.74 (**1e**H-4A/**1b**H-4A,**1c**H-4A) in the NOESY and ROESY spectra recorded at 300 K. These weak exchange peaks were not observed in the NOESY and ROESY spectra recorded at 271 K, indicating temperature-dependent reaction rates. Thus, the flavylium form may be an intermediate in the transition from **1d** and **1e** to the hemiacetal forms (**1b** and **1c**). The NMR spectral data (Table 4) did not contain sufficient information to differentiate between homologous signals of each of the two forms,

Table 2
^{1}H and ^{13}C NMR spectral data for the flavylium form of (malvidin 3-*O*-(6^{II}-*O*-α-rhamnopyranosyl^{AIV}-β-glucopyranoside^{AII})-5-*O*-β-glucopyranoside^{AIII}) (apigenin 6-*C*-(2^{II}-*O*-β-glucopyranosyl^{FIII}-β-glucopyranoside^{FII}) malonate^{AV} (A^{IV}-4 → A^{V}-1, F^{III}-6 → A^{V}-3), **1**, in CF_3COOD–CD_3OD (5:95; v/v) at 300 K

Malvidin	δ ^{1}H	δ ^{13}C[a]	Apigenin	δ ^{1}H	δ ^{13}C[a]
A2		164.0	F2		163.3[b]
A3		146.0	F3	6.90 *s*(*b*)[b]	103.8
A4	9.06 *s*	134.6	F4		180.8
A5		156.4	F5		nd
A6	7.13 *d*, 1.8	105.8	F6		113.1
A7		170.0	F7		nd
A8	7.24 *dd*, 1.8 0.9	97.4	F8	6.53 *s*(*b*)[c]	93.1
A9		157.6	F9		159.5[b]
A10		113.1	F10		107.3[b]
A1^{I}		119.6	F1^{I}		122.4 122.8
A2^{I}/6^{I}	8.11 *s*	110.8	F2^{I}/6^{I}	7.92 *'d'*, 8.7[c]	130.0
A3^{I}/5^{I}		149.9	F3^{I}/5^{I}	6.97 *'d'*, 8.6[c]	117.2[c]
A4^{I}		147.0	F4^{I}		168.3[b]
OMe	4.09 *s*	57.0			
A3-*O*-β-glucopyranoside			A5-*O*-β-glucopyranoside		
A1^{II}	5.57 *d*, 7.7 Hz	102.7	A1^{III}	5.27 *d*, 7.7 Hz	102.8
A2^{II}	3.77	74.6	A2^{III}	3.74	74.8
A3^{II}	3.66	78.4	A3^{III}	3.68	77.9
A4^{II}	3.53	71.4	A4^{III}	3.62	70.7
A5^{II}	3.89	77.5	A5^{III}	3.69	78.4
A6A^{II}	4.10	67.8	A6A^{III}	4.05 *dd*, 12.0, 2.2 Hz	62.3
A6B^{II}	3.75		A6B^{III}	3.90 *dd*, 12.0, 5.5 Hz	
A6^{II}-*O*-α-rhamnopyranosyl					
A1^{IV}	4.76 *d*, 1.5 Hz	102.2	A4^{IV}-*O*-malonyl		
A2^{IV}	3.84	71.8	A1^{V}		167.2
A3^{IV}	3.83	70.1	A2^{V}	3.44 *s*	[d]
A4^{IV}	4.87	76.5	A3^{V}		165.4
A5^{IV}	3.70	67.4			
A6^{IV}	0.99 *d*, 6.2 Hz	17.7			
F6-*C*-β-glucopyranoside			F2^{II}-*O*-β-glucopyranosyl		
F1^{II}	5.40 *d*, 10.3 Hz[b,c]	73.4	F1^{III}	4.49 *d*, 7.7 Hz	107.1
F2^{II}	4.43	84.1	F2^{III}	3.07	76.0
F3^{II}	3.79	82.5	F3^{III}	3.38 *t*, 9.5 Hz	77.6
F4^{II}	3.61	71.5	F4^{III}	3.25	70.4
F5^{II}	3.51	79.9	F5^{III}	3.23	74.8
F6A^{II}	3.95	62.7	F6A^{III}	4.14	64.6
F6B^{II}	3.80		F6B^{III}	4.07	

nd, not detected.
[a] Chemical shifts from the 1D CAPT and the 2D HSQC and HMBC NMR spectra.
[b] Chemical shifts/coupling constants from NMR spectra recorded at 271 K.
[c] Broad/duplicated signals caused by rotational conformers of the flavone unit.
[d] Exchange with deuterium.

1d and **1e**. They occurred in similar quantities, and their aromatic proton signals were very broad preventing observations of long-range correlations in the HMBC spectrum. These broad signals may indicate that the potential quinonoidal bases were involved in non-covalent inter- or intramolecular association structures. They may alternatively be caused by relatively rapid proton exchange between **1d** and **1e**, or they may reveal the occurrence of rotamers as observed for *C*-glycosylflavones with bulky *C*-substituents (Rayyan et al., 2005). The ^{1}H NMR signals of the flavylium cation (**1a**) were relatively sharp (Fig. 4), indicating slower proton exchange between the potential quinonoidal bases (**1d** and **1e**) and the flavylium form in acidified deuterated methanol than observed in D_2O.

2.4. Proportions of the various forms of *1* during storage

The relative proportions of the various forms of **1** (**1a**–**1e**) dissolved in acidified deuterated methanol varied with storage time (Fig. 7). Significant amounts of other species than **1a**–**1e** were not detected in the NMR spectra during the storage time (Fig. 4). In the 1D ^{1}H NMR spectrum recorded 45 min after sample preparation, **1** occurred mainly as potential quinonoidal bases (**1d**–**1e**) and flavylium cation (**1a**) (Fig. 7), whereas only minor amounts of the

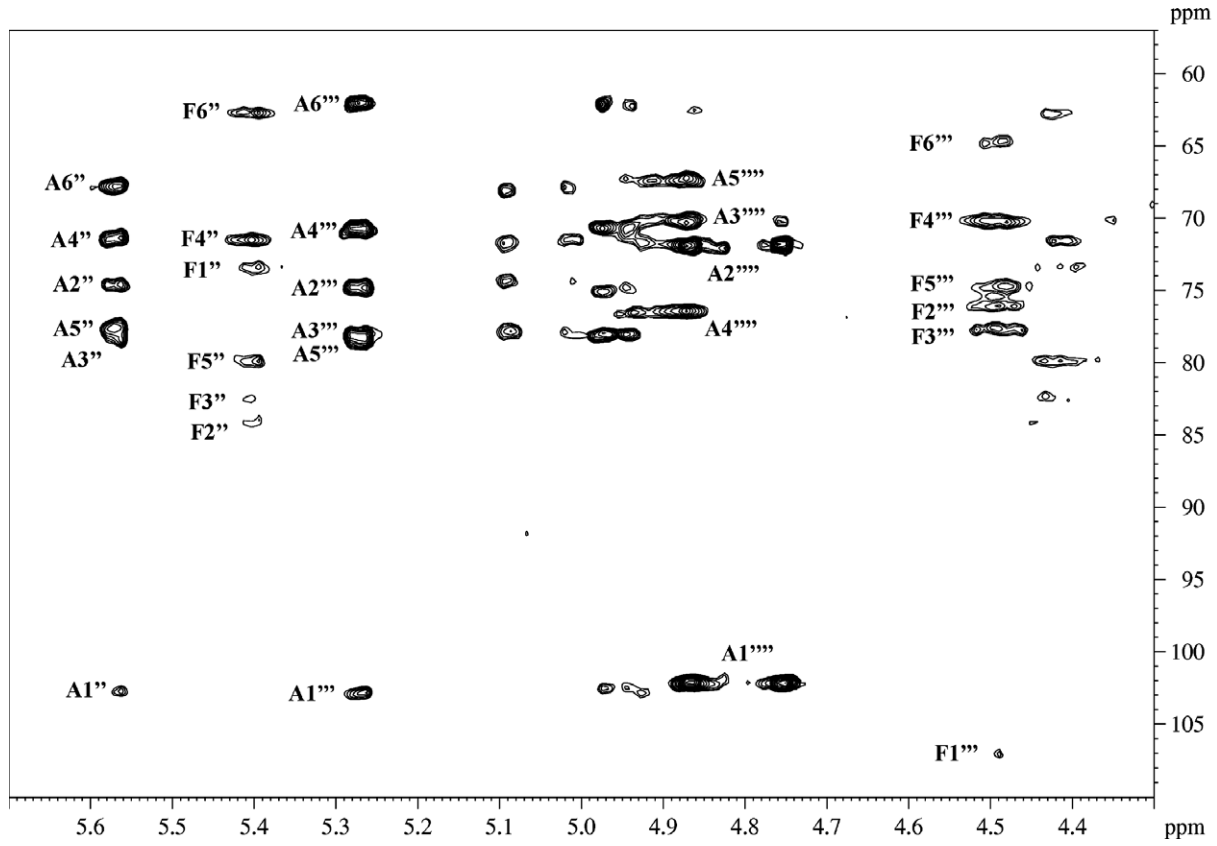

Fig. 5. Expanded region of the 2D ^{1}H–^{13}C HSQC-TOCSY spectrum of **1** showing assignments of ^{13}C resonances belonging to the sugar units of the flavylium cation form (**1a**). The methyl group of the rhamnosyl unit (A6‴′) is not included in this expansion.

hemiacetal forms (**1b**–**1c**) were present. The reduction of the amounts of the potential quinonoidal bases during storage correlated with an increase in the relative proportions of the colourless hemiacetal forms (Fig. 7). After five days storage the hemiacetal forms were the main forms of **1**. The relative proportions of the flavylium form were relatively stable throughout the storage period. In acidified deuterated methanolic solutions, solvents typically used for NMR analysis of anthocyanins, the anthocyanins have in literature mainly been considered to be on the flavylium cation form (Fossen and Andersen, 2006). Dissolved in CF_3CO_2D–CD_3OD (5:95), the proportion of the flavylium form of **1** constituted 40% (or slightly less).

In the 2D NOESY and ROESY spectra recorded at 300 K weak exchange crosspeaks at δ 9.06/6.54 and δ 9.06/6.57 involving H-4 of the flavylium form were observed. The chemical shifts at δ 6.54 and δ 6.57 may represent H-4 of two enantiomeric C-4 hydroxylated hemiacetal forms, as indicated by Mistry et al. (1991). In previous studies on equilibrium forms of anthocyanins, chalcone forms have been tentatively identified and their relative proportions were considered to increase with decreasing proportions of the flavylium cation (Mistry et al., 1991; Santos et al., 1993; Bakker et al., 1997). We cannot exclude the presence of chalcone forms in the examined sample. However, proton signals which could correspond to significant amounts of chalcone forms were not detected in any NMR spectrum of **1**.

2.5. Association structures involving equilibrium forms of *1*

In comparison with spectra of analogous monomeric anthocyanins, bathochromic shifts in UV–Vis spectra and observation of upfield chemical shifts (in particular that of anthocyanidin H-4) in ^{1}H NMR spectra of anthocyanin–flavonoid complexes, have been related to inter- or intramolecular copigmentation, presumably caused by vertical ‘π–π’ stacking of the anthocyanidin and the flavone/flavonol substituent (Toki et al., 1994, 2004; Bloor and Falshaw, 2000; Fossen et al., 2000). The visible absorption maxima in the UV–Vis spectrum of **1** recorded on-line during HPLC analysis showed a significant bathochromic shift (25 nm) compared to the analogous value of the similar monomeric anthocyanin malvidin 3-*O*-(6-*O*-(4-*O*-malonyl-α-rhamnopyranosyl-β-glucopyranoside)-5-*O*-β-glucopyranoside (**3**) without the flavone moiety (Table 1). However, the ^{1}H chemical shifts of the flavylium form of **1** were very similar to those of the flavylium form of **3** (Fossen et al., 2005), indicating that the flavone moiety of the flavylium form of **1** was not significantly involved in inter- or intra-molecular copigmentation. Neither was any crosspeak observed in the NOESY spectrum corresponding to

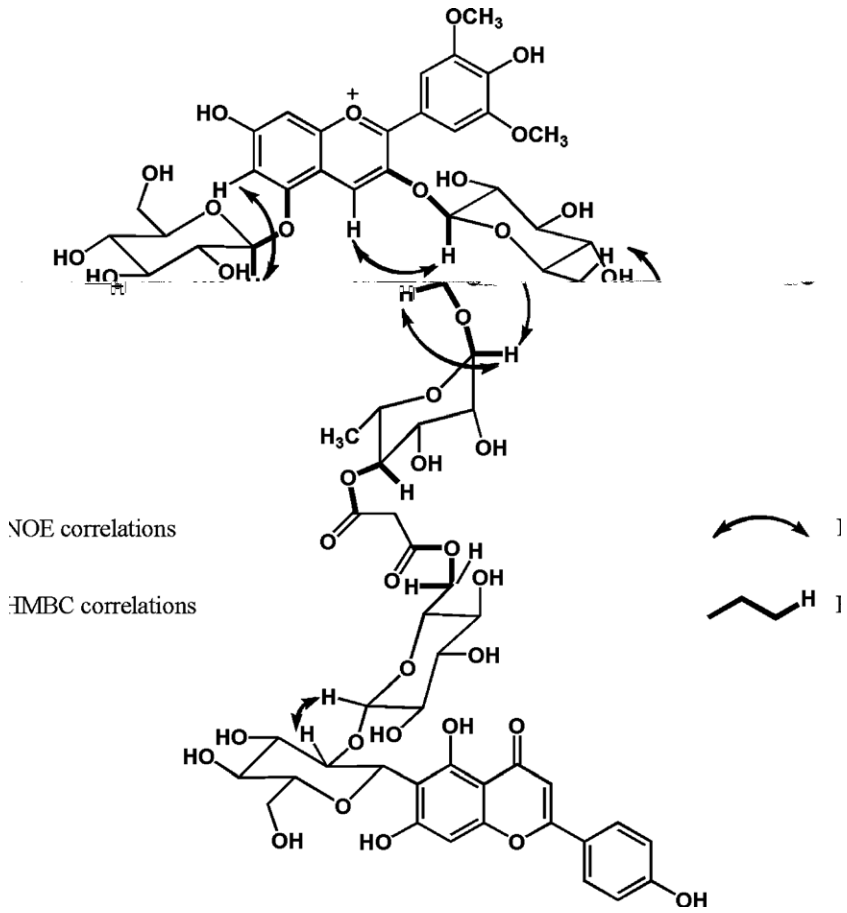

Fig. 6. Important NOE and HMBC correlations of (malvidin 3-*O*-(6^{II}-*O*-α-rhamnopyranosyl^{AIV}-β-glucopyranoside^{AII})-5-*O*-β-glucopyranoside^{AIII}) (apigenin 6-*C*-(2^{II}-*O*-β-glucopyranosyl^{FIII}-β-glucopyranoside^{FII}) malonate^{AV} (A^{IV}-4 → A^{V}-1, F^{III}-6 → A^{V}-3), **1**.

inter- or intramolecular association involving the flavylium form (**1a**) nor the hemicatal forms (**1b**–**1c**), even though some of these potential signals may be overlooked in this crowded spectrum. On the other hand four cross-peaks at *δ* 7.92/6.43, *δ* 7.92/6.22, *δ* 7.69/6.43 and *δ* 7.69/6.22 were observed. These cross-peaks revealed a close contact through space between **1d/1e**H-2′,6′F/**1d**H-6A and **1d/1e**H-2′,6′F/**1e**H-6A, respectively, indicating the presence of vertical 'π–π' stacking of the B-ring of the flavone unit and the A-ring of the anthocyanidin of **1d** and **1e**. It was not possible to discriminate between inter- or intramolecular association mechanisms. Previous studies of self-association of quinonoidal base equilibrium forms of malvidin 3,5-diglucoside in weakly acidic-neutral aqueous solutions using CD and ^{1}H NMR spectroscopy (Hoshino et al., 1982; Hoshino, 1991) have indicated a multimeric left-handed helical stacking geometry (Hoshino, 1991), wherein the vertical stack geometry of each pair of monomeric anthocyanidin sub-unit were proposed to be head-to-head or head-to-tail (Hoshino et al., 1982; Hoshino, 1991). Using CD, UV and NMR spectroscopy, self-association of the flavone flavocommelin related to solvent and sample concentration has been extensively studied (Goto et al., 1990). Association structures involving vertical stacking of quinonoidal bases and flavones have previously been reported for the non-covalent metalloanthocyanins Protocyanin (Kondo et al., 1998) and Commelinin (Goto and Kondo, 1991; Kondo et al., 1992), both dissolved in D_2O.

Table 3
^{1}H and ^{13}C NMR spectral data for the anthocyanidin part of the hemiacetal forms of **1** in CF_3COOD–CD_3OD (5:95; v/v) at 300 K (**1b** and **1c** are the minor and major form, respectively)

Malvidin	**1b**		**1c**	
	δ ^{1}H	*δ* ^{13}C[a]	*δ* ^{1}H	*δ* ^{13}C[a]
A2		103.2		103.2
A3		145.5		145.0
A4	6.72 *s*	98.8	6.71 *d*, 0.9 Hz	98.6
A5		154.0		154.5
A6	6.39 *d*, 1.8 Hz	97.9	6.37 *d*, 1.8 Hz	97.8
A7		157.9		158.2
A8	6.22 *dd*, 1.8 Hz, 0.9 Hz	97.9	6.20 *dd*, 1.8 Hz, 0.9 Hz	97.7
A9		153.0		152.5
A10		104.2		103.6
A1^{I}		131.7		132.4
A2^{I}/6^{I}	6.95 *s*	105.6	6.94 *s*	105.5
A3^{I}/5^{I}		148.5		148.5
A4^{I}		136.7		137.0
OMe	3.90 *s*	57.0	3.89 *s*	57.0

[a] Chemical shifts from the 2D HSQC and HMBC NMR spectra.

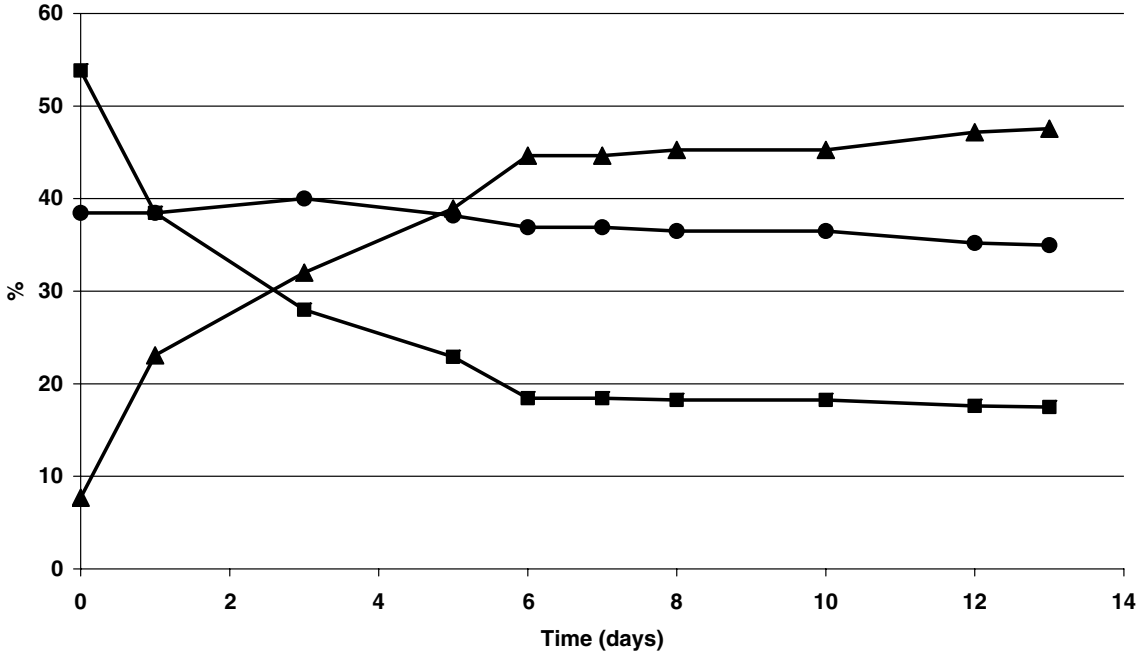

Fig. 7. Relative quantities of equilibrium forms of **1** derived from integration of the 1D ^{1}H NMR spectra recorded at different storage times at 300 K. Other compounds occurring in minor amounts have not been included in the calculations. Circles denote the flavylium form, squares denote the sum of the two forms assigned to quinonoidal bases, and triangles denote the sum of the two hemiacetal forms, respectively.

Table 4
^{1}H and ^{13}C NMR spectral data [a] identified for the two equilibrium forms assigned to be quinonoidal bases (**1d** and **1e**, respectively) of (malvidin 3-*O*-(6^{II}-*O*-α-rhamnopyranosyl^{AIV}-β-glucopyranoside^{AII})-5-*O*-β-glucopyranoside^{AIII}) (apigenin 6-*C*-(2^{II}-*O*-β-glucopyranosyl^{FIII}-β-glucopyranoside^{FII}) malonate^{AV} (A^{IV}-4 → A^{V}-1, F^{III}-6 → A^{V}-3) in CF_3COOD-CD_3OD (5:95; v/v) at 300 K

Malvidin	δ ^{1}H	δ ^{13}C[b]	Apigenin	δ ^{1}H	δ ^{13}C[b]
A4	8.97	133.0	F2′/6′	7.92	[c]
	8.92	131.0		7.69	129.4
A6	6.43	104.3	F3′/5′	6.91	117.0
	6.22	102.5		6.91	117.0
A8	6.29	95.1	A3-*O*-β-glucopyranoside		
	5.71	94.5			
A2′/6′	7.77	110.5	1″	5.91	100.1
	7.64	110.2		5.56	102.8
OCH_3	4.03	[c]			
	4.03	[c]			

[a] Homologous signals could not be assigned specifically to either **1d** or **1e**.
[b] Chemical shifts from the 2D HSQC NMR spectrum.
[c] In crowded region.

3. Experimental

3.1. Isolation of pigments

Purple shamrock (*Oxalis triangularis*) was cultivated in Bergen. A voucher specimen has been deposited in Bergen Herbarium, University of Bergen (accession number H/505).

Leaves (100 g) were cut into pieces and extracted (2 times) with 0.5% TFA in MeOH at 4 °C. The filtered extract was concentrated under reduced pressure, purified by partition against EtOAc (equal volume, three times), and then subjected to Amberlite XAD-7 column chromatography (Goto et al., 1982; Andersen, 1988). Pigment **1** was separated from the monomeric anthocyanins by Sephadex LH-20 column chromatography (100 × 5 cm) using MeOH–H_2O–TFA (19.8:80:0.2; v/v) as mobile phase. The flow rate was 2.5 ml min^{-1}. Prior to elution of the fraction containing **1** (245 ml), 665 ml of the mobile phase was eluted. Pigment **1** was then purified by preparative HPLC.

Preparative HPLC (Gilson 305/306 pump equipped with an HP-1040A detector) was performed with an ODS-Hypersil column (25 × 2.2 cm, 5 μm) using the solvents HCOOH–H_2O (1:18, v/v) (A) and HCOOH–H_2O–MeOH (1:8:10, v/v) (B). The elution profile consisted of a linear gradient from 10% B to 100% B for 45 min, isocratic elution (100% B) for the next 13 min, followed by linear gradient from 100% B to 10% B for 1 min. The flow rate was 14 ml min^{-1}, and aliquots of 300 μl were injected. Five milligram of pigment **1** were isolated.

3.2. Analytical HPLC

Analytical HPLC was performed with an ODS-Hypersil column (25 × 0.3 cm, 5 μm) using the solvents HCOOH–H_2O (1:18) (A) and HCOOH–H_2O–MeOH (1:8:10) (B). The gradient consisted of a linear gradient from 10% B to 100% B for 23 min, 100% B for the next 5 min, followed by linear gradient from 100% B to 10% B for 1 min. The flow rate was 0.75 ml min^{-1}, and aliquots of 15 μl were injected.

3.3. Spectroscopy

UV–Vis absorption spectra were recorded in 0.01% HCl–MeOH and on-line during HPLC analysis over the wavelength range 240–600 nm in steps of 2 nm (Fig. 2). UV–Vis data of **1** in 0.01% HCl–MeOH: Vis-max: 544 nm; UV-max: 347 nm, 302 nm, 278 nm; $A_{440}/A_{\text{vis-max}}$: 12%.

The 1D ^{1}H and the 2D HSQC, HSQC-TOCSY, HMBC, TOCSY, NOESY, ROESY and DQF-COSY NMR experiments were obtained at 600.13 MHz and 150.90 MHz for ^{1}H and ^{13}C, respectively, on a Bruker 600 MHz instrument equipped with a cryogenic probe. Sample temperatures were stabilized at 300 K. A 2D ROESY NMR experiment was also recorded at 271 K and 2D NOESY NMR experiments were additionally recorded at 271 K and 277 K, respectively. The deuteriomethyl ^{13}C signal and the residual ^{1}H signal of the solvent (CF_3CO_2D–CD_3OD; 5:95, v/v) were used as secondary references (δ 49.0 and δ 3.40 from TMS, respectively). The concentration of the NMR sample of **1** was 1.5 mM.

Electrospray mass spectrometry was performed at Helmholz Centre for Infection Research, Department of Structural Biology (Braunschweig, Germany). The pigment was dissolved in a 1:1 (v/v) methanol/1% formic acid solution. Approximately 3 μl of this solution (final concentration ca. 20 pmol/l) was filled into a gold-coated nanospray glass capillary (Protana, Odense, Denmark). The tip of the capillary was placed orthogonally in front of the entrance hole of a quadrupole time-of-flight (QTOF 2) mass spectrometer (Micromass, Manchester, Great Britain) equipped with a nanospray ion source, and a voltage of approximately 1000 V was applied. For collision-induced dissociation experiments, parent ions were selectively transmitted from the quadrupole mass analyser into the collision cell. Argon was used as the collision gas and the kinetic energy was set at around 25 eV. The resulting daughter ions were then separated by the orthogonal time-of-flight mass analyser.

Acknowledgements

The authors are grateful to Professor Dag Olav Øvstedal, Department of Botany, University of Bergen, for identification of *Oxalis triangularis*, Mrs. Solrunn Marie Fosse for providing the original plant material, Mrs. Undine Felgenträger, Helmholz Centre for Infection Research, Department of Structural Biology (Braunschweig, Germany) for recording the high resolution electrospray mass spectra, and The Norwegian Research Council (NFR) for support. T.F. and S.R. gratefully acknowledge NFR and The State Education Loan Fund, respectively, for their fellowships.

References

Andersen, Ø.M., 1988. Semipreparative isolation and structure determination of pelargonidin 3-*O*-α-L-rhamnopyranosyl-(1 → 2)-β-D-glucopyranoside and other anthocyanins from the tree *Dacrycarpus dacrydioides*. Acta Chem. Scand. 42, 462–468.

Andersen, Ø.M., Jordheim, M., 2006. The anthocyanins. In: Andersen, Ø.M., Markham, K.R. (Eds.), Flavonoids: Chemistry, Biochemistry and Applications. CRC Press, Boca Raton, pp. 471–551.

Bakker, J., Timberlake, C.F., 1997. Isolation, identification and characterization of new color-stable anthocyanins occurring in some red wines. J. Agric. Food Chem. 45, 35–43.

Bakker, J., Bridle, P., Honda, T., Kuwano, H., Saito, N., Terahara, N., Timberlake, C.F., 1997. Identification of an anthocyanin occurring in some red wines. Phytochemistry 44, 1375–1382.

Bloor, S.J., Falshaw, R., 2000. Covalently linked anthocyanin–flavonol pigments from blue *Agapanthus* flowers. Phytochemistry 53, 575–579.

Brouillard, R., Dangles, O., 1994. Flavonoids and flower colour. In: Harborne, J.B. (Ed.), The Flavonoids, Advances in Research Since 1986. Chapman & Hall, London, pp. 565–588.

Cheminat, A., Brouillard, R., 1986. PMR investigation of 3-*O*-(β-D-glucosyl)malvidin structural transformations in aqueous solutions. Tetrahedron Lett. 27, 4457–4460.

Figueiredo, P., Elhabiri, M., Toki, K., Saito, N., Dangles, O., Brouillard, R., 1996. New aspects of anthocyanin complexation. Intramolecular copigmentation as a means for colour loss? Phytochemistry 41, 301–308.

Fossen, T., Andersen, Ø.M., 2003. Anthocyanins from red onion, *Allium cepa*, with novel aglycone. Phytochemistry 62, 1217–1220.

Fossen, T., Andersen, Ø.M., 2006. Spectroscopic techniques applied to flavonoids. In: Andersen, Ø.M., Markham, K.R. (Eds.), Flavonoids: Chemistry, Biochemistry and Applications. CRC Press, Boca Raton, pp. 37–142.

Fossen, T., Slimestad, R., Øvstedal, D.O., Andersen, Ø.M., 2000. Covalent anthocyanin–flavonol complexes from flowers of chive, *Allium schoenoprasum*. Phytochemistry 54, 317–323.

Fossen, T., Rayyan, S., Holmberg, M.H., Nateland, H.S., Andersen, Ø.M., 2005. Acylated anthocyanins from leaves of *Oxalis triangularis*. Phytochemistry 66, 1133–1140.

Fulcrand, H., Benabdeljalil, C., Rigaud, J., Cheynier, V., Moutounet, M., 1998. A new class of wine pigments generated by reaction between pyruvic acid and grape anthocyanins. Phytochemistry 47, 1401–1407.

Gakh, E.G., Dougall, D.K., Baker, D.C., 1998. Proton nuclear magnetic resonance studies of monoacylated anthocyanins from the wild carrot: Part 1. Inter- and intra-molecular interactions in solution. Phytochem. Anal. 9, 28–34.

Goto, T., Kondo, T., 1991. Structure and molecular stacking of anthocyanins – flower color variation. Angew. Chem. Int. Ed. 30, 17–33.

Goto, T., Kondo, T., Tamura, H., Imagawa, H., Iino, A., Takeda, K., 1982. Structure of gentiodelphin, an acylated anthocyanin isolated from *Gentiana Makinoi*, that is stable in dilute aqueous solution. Tetrahedron Lett. 23, 3695–3698.

Goto, T., Tamura, H., Kondo, T., 1987. Chiral stacking of cyanin and pelargonin – soluble and insoluble aggregates as determined by means of circular dichroism. Tetrahedron Lett. 28, 5907–5908.

Goto, T., Yoshida, K., Yoshikane, M., Kondo, T., 1990. Chiral stacking of a natural flavone, flavocommelin, in aqueous solution. Tetrahedron Lett. 31, 713–716.

Hoshino, T., 1991. An approximate estimate of self-association constants and the self-stacking conformation of malvidin quinonoidal bases studied by ^{1}H NMR. Phytochemistry 30, 2049–2055.

Hoshino, T., 1992. Self-association of flavylium cations of anthocyanidin 3,5-diglucosides studied by circular dichroism and ^{1}H NMR. Phytochemistry 31, 647–653.

Hoshino, T., Matsumoto, U., Goto, T., Harada, N., 1982. Evidence for the self-association of anthocyanins IV. PMR spectroscopic evidence for the vertical stacking of anthocyanin molecules. Tetrahedron Lett. 23, 433–436.

Kondo, T., Yoshida, K., Nakagawa, A., Kawai, T., Tamura, H., Goto, T., 1992. Structural basis of blue-colour development in flower petals from *Commelina communis*. Nature 358, 515–518.

Kondo, T., Ueda, M., Isobe, M., Goto, T., 1998. A new molecular mechanism of blue color development with protocyanin, a supramolecular pigment from cornflower, *Centaurea cyanus*. Tetrahedron Lett. 39, 8307–8310.

Mistry, T.V., Cai, Y., Lilley, T.H., Haslam, E., 1991. Polyphenol interactions. Part 5. Anthocyanin copigmentation. J. Chem. Soc. Perkin Trans. 2, 1287–1296.

Nerdal, W., Andersen, Ø.M., 1991. Evidence for self-association of the anthocyanin petain in acidified, methanolic solution using two-dimensional nuclear overhauser enhancement NMR experiments and distance geometry calculations. Phytochem. Anal. 2, 263–270.

Nerdal, W., Andersen, Ø.M., 1992. Intermolecular aromatic acid association of an anthocyanin (Petanin) evidenced by 2-dimensional nuclear Overhauser enhancement nuclear-magnetic-resonance experiments and distance geometry calculations. Phytochem. Anal. 3, 182–189.

Rayyan, S., Fossen, T., Andersen, Ø.M., 2005. Flavone C-glycosides from leaves of *Oxalis triangularis*. J. Agric. Food Chem. 53, 10057–10060.

Santos, H., Turner, D.L., Lima, J.C., Figueiredo, P., Pina, F.S., Macanita, A.L., 1993. Elucidation of the multiple equilibria of malvin in aqueous solution by one- and two-dimensional NMR. Phytochemistry 33, 1227–1232.

Strack, D., Busch, E., Klein, E., 1989. Anthocyanin patterns in european orchids and their taxonomic and phylogenetic relevance. Phytochemistry 28, 2127–2139.

Takeda, K., Harborne, J.B., Waterman, P.G., 1993. Malonylated flavonoids and blue flower colour in lupin. Phytochemistry 34, 421–423.

Takeda, K., Yanagisawa, M., Kifune, T., Kinoshita, T., Timberlake, C.F., 1994. A blue pigment complex in flowers of Salvia patens. Phytochemistry 35, 1167–1169.

Terahara, N., Suzuki, H., 1993. A diacylated anthocyanin from *Tibouchina urvilleana* flowers. J. Nat. Prod. 56, 335–340.

Toki, K., Saito, N., Iimura, K., Suzuki, T., Honda, T., 1994. (Delphinidin 3-gentiobiosyl) (apigenin 7-glucosyl) malonate from the flowers of *Eichhornia crassipes*. Phytochemistry 36, 1181–1183.

Toki, K., Saito, N., Tsutsumi, S., Tamura, C., Shighihara, A., Honda, T., 2004. (Delphinidin 3-gentiobiosyl) (luteolin 7-glucosyl) malonate from the flowers of *Eichhornia crassipes*. Heterocycles 63, 899–902.